2017 SNMMI Highlights Lecture: Cardiovascular Nuclear Medicine

Nagara Tamaki, MD, PhD, Hokkaido University, Sapporo, Japan; and Kyoto Prefectural University of Medicine, Kyoto, Japan

From the Newsline Editor: The Highlights Lecture, presented at the closing session of each SNMMI Annual Meeting, was originated and presented for more than 30 years by Henry N. Wagner, Jr., MD. Beginning in 2010, the duties of summarizing selected significant presentations at the meeting were divided annually among 4 distinguished nuclear and molecular medicine subject matter experts. Each year Newsline publishes these lectures and selected images. The 2017 Highlights Lectures were delivered on June 14 at the SNMMI Annual Meeting in Denver, CO. In this issue we feature the lecture by Nagara Tamaki, a professor at Hokkaido University (Sapporo, Japan) and Kyoto Prefectural University of Medicine (Kyoto, Japan), who spoke on highlights in cardiovascular nuclear medicine. Note that in the following presentation summary, numerals in brackets represent abstract numbers as published in The Journal of Nuclear Medicine *(2017;58[suppl 1]).*

Many interesting and valuable studies were presented in cardiovascular and related sessions at the SNMMI 2017 Annual Meeting. The number of abstracts on cardiovascular topics presented at this year's meeting (115) was slightly reduced in comparison to 2016 and 2015 (120 and 123, respectively). The quality of the abstracts, however, remains high. The geographic distribution of abstract submissions changed from 2016 to 2017, with significant increases in those coming from North America (34 to 61) and fewer from Europe (46 to 18) and Asia (40 to 36). The reduction in the number of abstracts from Europe might be explained by the calendar proximity of the International Congress of Nuclear Cardiology and Cardiac CT, held May 7–9 in Vienna, Austria, with many high-quality abstracts already presented.

As in 2016, presentations at SNMMI in 2017 showed a shift away from myocardial perfusion imaging toward molecular imaging in both basic and clinical sciences. This trend was nicely demonstrated at the Cardiovascular Young Investigator Award Symposium, which featured presentations on imaging of atherosclerosis, neuronal activity, amyloidosis, and sarcoidosis. Sharmila Dorbara, MD, in the 2017 Hermann Blumgart Lecture, emphasized and summarized the importance of expanding the frontiers of nuclear cardiology, particularly for infiltrative cardiomyopathy, one of the most challenging areas.

Assessment of Atherosclerosis

Among various possible targets and ligands for imaging atherosclerosis, ^{18}F-FDG and ^{18}F-NaF have been most commonly used in basic science investigations as well as in clinical settings.

Nagara Tamaki, MD, PhD

Castro et al. from the Hospital of the University of Pennsylvania (Philadelphia) and Odense University Hospital (Denmark) reported that "Common carotid artery molecular calcification assessed by ^{18}F-NaF PET/CT is associated with increased cardiovascular disease risk: Results from the CAMONA study" [34]. Carotid ^{18}F-NaF uptake values (SUV_{max} and SUV_{mean}) were used to successfully identify patients with high risk of cardiovascular events. Furthermore, a linear relationship was observed between ^{18}F-NaF uptake and 10-year estimated risk of cardiovascular events. The authors concluded that these results suggest that "^{18}F-NaF PET/CT can provide a valuable tool for predicting cardiovascular events."

Nakahara et al. from the Icahn School of Medicine at Mount Sinai (New York, NY) and the Memorial Sloan Kettering Cancer Center (New York, NY) reported on "The relationship between ^{18}F-NaF and calcium on the time course of vascular calcification" [444] in patients with prostate cancer. Figure 1 shows a typical example of the time course of NaF uptake and aortic calcification, indicating that vascular uptake on PET may predict calcification volume changes 1−1.5 years later. This important work illuminates the mechanistic basis of atherosclerotic plaque calcification, vascular ^{18}F-NaF uptake, and calcium volume in the thoracic and abdominal aorta on serial scans.

Various new molecular markers have been introduced for atherosclerosis imaging in both translational and clinical studies. Li et al. from the Medical University of Vienna (Austria) and Fuwai Hospital (Beijing, China) reported on "^{68}Ga-pentixafor PET/MRI for detection of chemokine receptor 4 (CXCR4) expression in atherosclerotic plaque" [297]. Figure 2 shows representative images of carotid ^{68}Ga-pentixafor PET/MR images from 4 types of arterial lesions in oncology patients. ^{68}Ga-pentixafor uptake in carotid atherosclerotic lesions is significantly higher than that in normal carotid arteries. In atherosclerotic lesions, this uptake is more intense in intermediate plaques (type 2) and advanced atheromatous/fibrous atheromatous plaques (type 3) than in fibrocalcific plaques (type 4). These data indicate that CXCR4 is higher in atheromatous or fibrous atheromatous lesions with lipid-rich necrotic cores than in fibrocalcific plaque in carotid atherosclerotic lesions. The authors concluded that quantification of ^{68}Ga-pentixafor uptake on PET, with dedicated MR imaging analyses of the vessel wall, might be useful in clinical characterization of atherosclerosis.

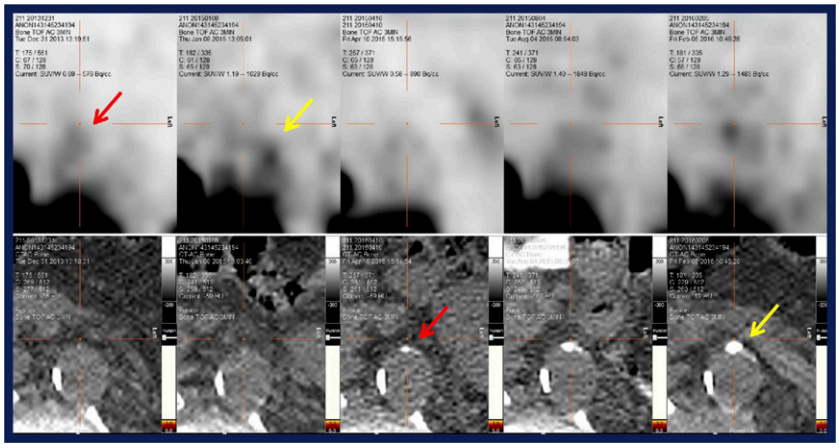

FIGURE 1. Typical example of PET imaging of the time course of ^{18}F-NaF uptake (top) and aortic calcification (bottom) of the abdominal aorta in a 76-year-old patient with hypertension and prostatic cancer. Vascular ^{18}F-NaF uptake (arrows) may be related to an increase in calcified volume (arrows) over 1–2-year follow-up, indicating that ^{18}F-NaF vascular uptake may predict future calcification volume change 1–1.5 years after imaging.

Sultan et al. from the Washington University School of Medicine (St. Louis, MO), Mallinckrodt Institute of Radiology (St. Louis, MO), and the University of California Santa Barbara reported on "Chemokine receptor CCR5 targeted nanoparticle imaging of atherosclerosis with PET" [161]. The researchers used ^{64}Cu-DAPTA-Comb in a mouse ApoE−/− model of atherosclerosis and studied disease regression after treatment with an adeno-associated virus vector (AAV) carrying ApoE and clodronate, which removes circulating monocytes. Three weeks after AAV treatment, ^{64}Cu-DAPTA-Comb PET imaging showed reduced signal in the treated mice, although plaque size was slightly but not significantly reduced. Cholesterol levels dropped within the first week of treatment and remained low compared to levels in untreated mice (Fig. 3). They concluded that ^{64}Cu-DAPTA-Comb effectively detected a drop in monocytes following treatment. A number of similar reports suggest that molecular markers are valuable not only for identifying vulnerable plaque but also for monitoring atheroma progression or regression with various treatments.

Johnson et al. from Columbia University and Columbia University Medical Center (New York, NY) and SibTech, Inc. (Brookfield, CT) reported on "Dual-isotope hybrid SPECT/CT in a porcine model of peripheral artery disease" [164] using ^{201}Tl and ^{99m}Tc-scVEGF-PEG-DOTA (scV/Tc). ^{201}Tl SPECT/CT hindlimb imaging in minipigs documented reduced perfusion to the vascular territory of ligated arterial vessels immediately after ligation as well as improved flow and formation of collaterals at day 28 (Fig. 4). scV/Tc focal uptake was seen at the ligation site (Fig. 5). The source of signal from high vascular endothelial growth factor expression was correlated with angiogenic response to both hypoxia and wound healing from the incision. This study nicely showed the value of dual-isotope hybrid SPECT/CT imaging for perfusion and angiogenesis in this peripheral arterial ligation model. The authors also emphasized the potential of this technique in clinical imaging to assess therapies aimed at improving blood flow in patients with peripheral artery disease.

Another elegant study in peripheral artery disease was reported by Bankstahl et al. from the Hannover Medical

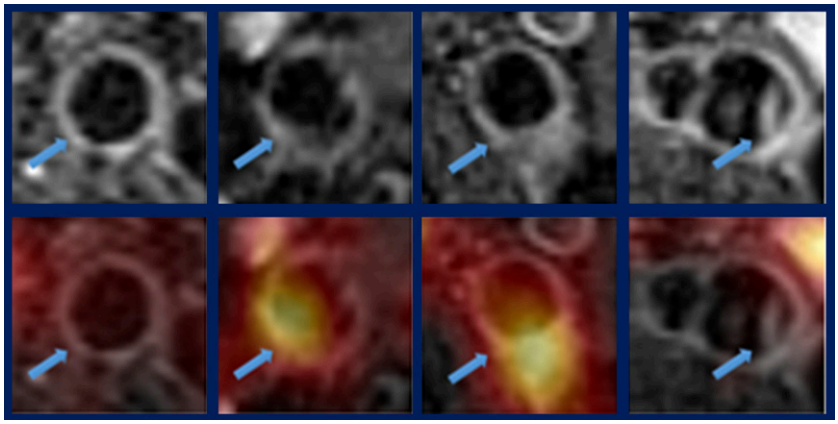

FIGURE 2. Representative images of carotid MR (top row) and PET/MR (bottom row) imaging with ^{68}Ga-pentixafor, a novel PET tracer with an affinity to the chemokine receptor type 4 protein (CXCR4) in a study of oncology patients. Tracer uptake was seen in the carotid artery (arrows). Atherosclerotic lesions were classified into 4 types based on MR findings and quantified PET tracer uptake: (left to right) type 1, normal common carotid artery; type 2, atherosclerotic carotid artery with intermediate eccentric thickening; type 3, carotid atheromatous or fibrous atheromatous plaques with lipid-rich necrotic core; and type 4, fibrocalcific plaques. ^{68}Ga-pentixafor uptake in carotid atherosclerotic lesions was significant higher than in normal carotid lesions. In atherosclerotic lesions, ^{68}Ga-pentixafor uptake presented more intensively in intermediate eccentric thickening plaques (type 2) and advanced atheromatous/fibrous atheromatous plaques (type 3) than in fibrocalcific plaques (type 4).

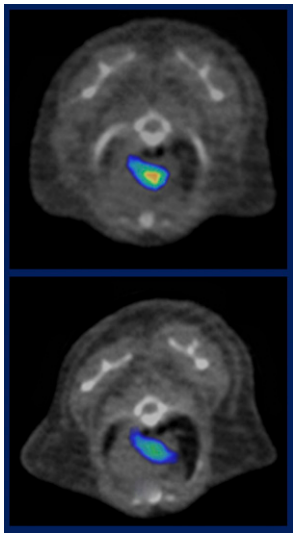

FIGURE 3. ^{64}Cu-DAPTA-Comb chemokine receptor peptide antagonist CCR5-targeted nanoparticle PET imaging in an atherosclerosis mouse ApoE−/−model (top). After treatment with adeno-associated virus vector carrying ApoE and clodronate (bottom), ^{64}Cu-DAPTA-Comb imaging showed reduced signal in the treated mice, although plaque size was slightly but not significantly reduced. Cholesterol levels dropped within the first week of treatment and remained low compared to those in untreated mice.

School (Germany), who reported on "Multitracer characterization of ischemic inflammation and perfusion in a murine model of hindlimb ischemia" [32]. The authors characterized various biologic events, including perfusion deficits, metabolic response, inflammation, angiogenesis, and functional recovery (Fig. 6). They reported that multimodal imaging reveals massive early ischemia-induced inflammation after peripheral artery occlusion, followed by a phase of perfusion recovery and angiogenesis, showing a close interaction between inflammation and perfusion changes. In the study of peripheral vascular disease, perfusion, metabolism, and angiogenesis may be used as important biomarkers for severity assessment and treatment monitoring.

Assessment of Myocardial Dysfunction

A number of studies focused on myocardial dysfunction using various molecular probes. I would like to focus on 2 presentations on the identification of acute inflammation after acute myocardial infarction (AMI). Derlin et al. from the Hannover Medical School (Germany) and the Technische Universität München (Garching, Germany) reported that "Regional CXCR4 upregulation in patients early after reperfused myocardial infarction is associated with systemic inflammation and left ventricular dysfunction" [97]. CXCR4 is a marker of leukocyte tissue infiltration, and, again, these authors used ^{68}Ga-pentixafor PET/CT to image its activity. They looked at CXCR4 upregulation (i.e., inflammation) early after AMI and its correlation with both left ventricular dysfunction at the time of imaging and with CXCR4 upregulation in other tissues, such as the spleen and vessel wall (Fig. 7). This study illustrates the ways in which inflammation networking plays a role in the response to early damage by AMI. The authors noted that such imaging may be useful for prediction of subsequent ventricular remodeling and for determining response to CXCR4-directed or other antiinflammatory treatment.

Taki et al. from Kanazawa University and Kanazawa University Hospital (Japan) and Mie University (Tsu, Japan) reported that "Postconditioning accelerates myocardial inflammatory resolution demonstrated by ^{14}C-methionine imaging and attenuates ventricular remodeling after severe ischemia and reperfusion" [160]. The left coronary artery was occluded in rats for 30 minutes followed by reperfusion. At reperfusion, postconditioning was achieved by 6 repeated episodes of 10-sec reperfusion, each followed by 10 seconds of occlusion. At 1, 3, 7, and 14 days after reperfusion, ^{14}C-methionine was injected 20 minutes before euthanasia. One minute before euthanasia, the left coronary artery was reoccluded and ^{99m}Tc-MIBI was injected to verify the area at risk. Post-mortem images of thallium perfusion and inflammatory marker ^{14}C-labeled methionine uptake showed lower methionine uptake and smaller perfusion defect with attenuated left ventricular remodeling at days 7 and 14 in the postconditioning group compared with a control group (Fig. 8). The authors concluded that postconditioning may accelerate recovery from the inflammatory process, based on the finding of reduction of both methionine uptake and ventricular remodeling

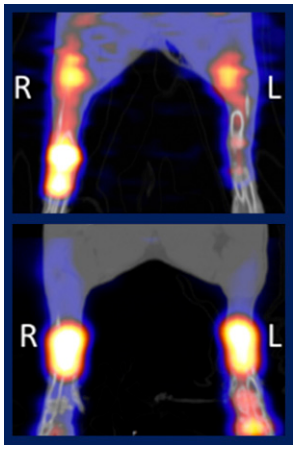

FIGURE 4. ^{201}Tl SPECT/CT hindlimb imaging at days 1 (top) and 28 (bottom) after left external femoral artery ligation in minipigs. Reduced perfusion to vascular territory at day 1 was noted after ligation, with improvement in flow and formation of collaterals at day 28.

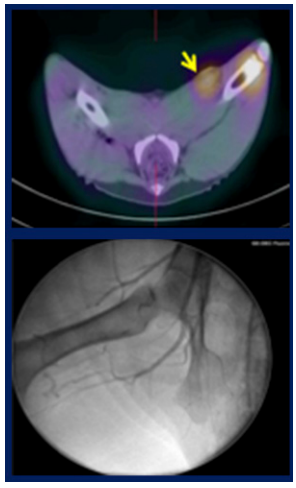

FIGURE 5. ^{99m}Tc-labeled scVEGF-PEG-DOTA (scV/Tc) scan at day 7 (top) showing the transverse section level of the semimembranosus in the same minipig model as Figure 4. scV/Tc focal uptake was seen at the ligation site (arrow), with higher tracer uptake in the wounded side (right) than the contralateral side. A high vascular endothelial growth factor expression may be related to angiographic response to hypoxia and to wound healing. Bottom image shows contrast angiography of the left leg at day 28.

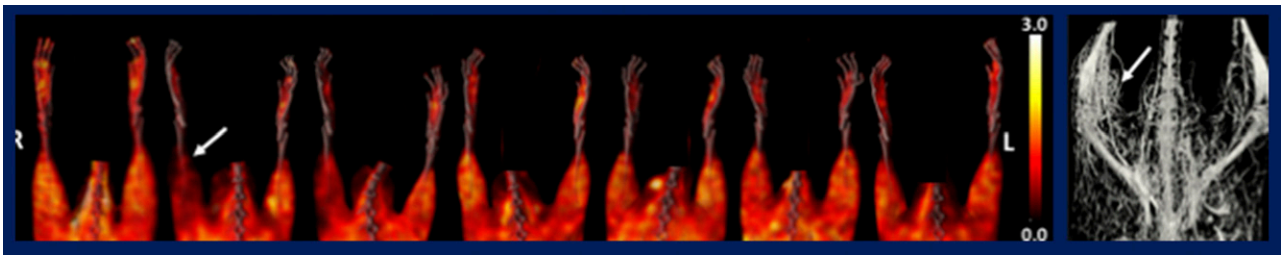

FIGURE 6. A hindlimb ischemia murine model was assessed with multiple tracers to characterize perfusion and various biologic events from early perfusion deficits to subsequent metabolic response. ^{99m}Tc-sestamibi SPECT imaging (color images) showed perfusion deficit changes from (left to right) baseline and at days 1, 3, 7, 10, 15, and 21, with unilateral femoral artery occlusion on day 1. Follow-up angiography at day 22 with bismuth chloride–enhanced CT (far right) shows collateral circulation (arrow). Perfusion reduction with gradual recovery was noted on ^{99m}Tc sestamibi and ^{99m}Tc-human serum albumin microsphere studies, with rapid and high accumulations of macrophage activation and angiogenesis tracers followed by glucose metabolism. This multitracer study nicely characterized the biologic events, including early perfusion deficits, subsequent metabolic response, inflammation, and later angiogenesis with functional recovery.

after myocardial infarction. In addition, methionine imaging may be useful for evaluation of postinfarction inflammatory change and prediction of left ventricular reverse remodeling.

Several reports at this meeting addressed the use of ^{18}F-FDG PET and MR imaging in cardiac sarcoidosis and other active myocardial disorders. In studying cardiac sarcoidosis with ^{18}F-FDG PET, many nuclear physicians struggle with the challenge of inhibiting physiologic FDG uptake sufficiently to differentiate it from abnormal uptake in active sarcoid lesions. Norikane et al. from Kagawa University and Kagawa University Hospital (Japan) reported on a "Comparative evaluation of ^{18}F-FLT PET/CT and ^{18}F-FDG PET/CT in patients with newly diagnosed thoracic sarcoidosis" [36]. A representative case showed positive uptake of both ^{18}F-FDG and ^{18}F-FLT in cardiac and pulmonary lesions (Fig. 9), suggesting that ^{18}F-FLT may be as effective as ^{18}F-FDG for detection of cardiac and pulmonary lesions. Although ^{18}F-FLT uptake values were significantly lower than those for ^{18}F-FDG, there were no inconclusive findings with ^{18}F-FLT PET/CT, compared to 4 inconclusive findings with ^{18}F-FDG PET/CT as a result of diffuse cardiac uptake. The authors concluded that ^{18}F-FLT PET/CT may be easier to perform because it does not require prolonged fasting and/or a special diet prior to imaging. A number of other imaging biomarkers have been suggested and are under investigation to identify active cardiac lesions, including cardiac sarcoidosis. Despite uptake with such tracers that is lower than that with ^{18}F-FDG, their uptake may be more specific for active myocardial lesions.

Bone marrow mesenchymal stem cell therapy remains a promising possibility for limiting infarct size and improving

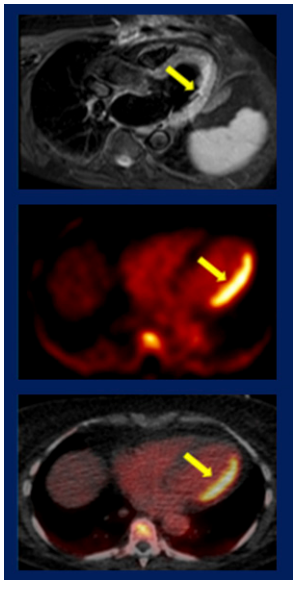

FIGURE 7. ^{68}Ga-pentixafor, a novel PET tracer with an affinity to chemokine receptor type 4 protein (CXCR4), in a patient early after myocardial infarction. Images include MR (top), PET (middle), and PET/CT (bottom). Tracer uptake was found to be higher in patients with reduced left ventricular ejection fraction (LVEF) than in a group with normal LVEF and to be inversely correlated with baseline LVEF. Moreover, myocardial CXCR4 uptake was significantly correlated with CXCR4 uptake in the aortic wall and spleen. This demonstrated the role of inflammation networking in response to early damage by acute myocardial infarction.

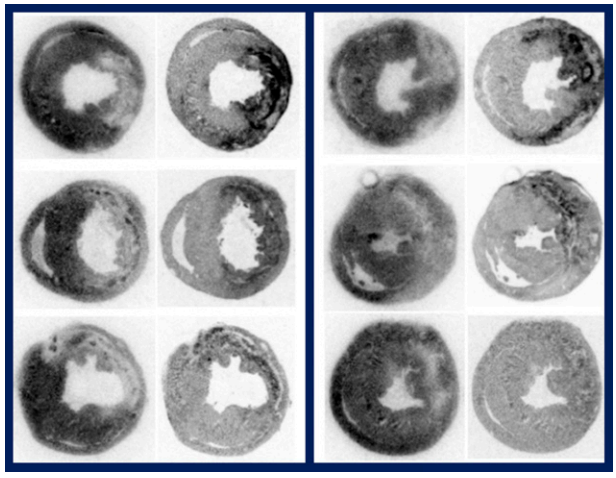

FIGURE 8. Ex vivo images in control (left block) and postconditioning (right block; 6 occlusion/reperfusion cycles) before left coronary artery occlusion in a rat model at (top to bottom) days 3, 7, and 14. Left column in each block shows ^{201}Tl perfusion; right column in each block shows uptake of the inflammatory marker ^{14}C-methionine. The postconditioning group showed lower ^{14}C-methionine uptake and less perfusion defect at days 7 and 14, indicating attenuated inflammation and left ventricular remodeling by postconditioning.

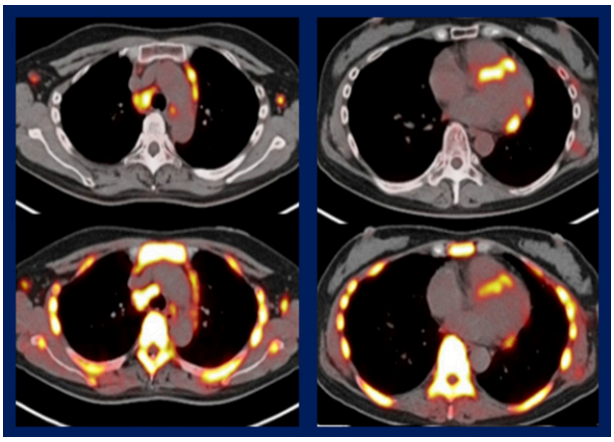

FIGURE 9. A representative case of ^{18}F-FDG PET/CT (top) and ^{18}F-fluorothymidine (^{18}F-FLT) PET/CT (bottom) in a patient with cardiopulmonary sarcoidosis. Both tracers accumulated nicely in pulmonary lymph nodes and cardiac lesions, although ^{18}F-FLT uptake was lower than that of ^{18}F-FDG in cardiac lesions.

cardiac function after AMI. Liu et al. from Union Hospital and Tongji Medical College at Huazhong University of Science and Technology (Wuhan, China) reported on "Using the tyrosinase gene as a trimodality reporter gene for monitoring transplanted stem cells in AMI" [167] in Sprague–Dawley rats. Figure 10 shows ^{18}F-5-fluoro-*N*-(2-[diethylamino]ethyl)pocolinamide (^{18}F-FPN) PET, MR, and photoacoustic imaging (PAI) of tyrosinase reporter gene bone-marrow mesenchymal stem cells (top) and control stem cells (bottom) at days 1, 7, 14, 21, and 28 after transplantation. Although prominent signals are seen with each modality, PET provided the best and most persistent positive findings compared with MR imaging or PAI. The advantages of each imaging modality in this setting must be considered. This study nicely showed that ^{18}F-5-FPN PET may be valuable for monitoring stem cell therapy over a long period of time.

Sympathetic neurotransmission imaging has been used in patients with heart failure and various myocardial disorders in order to identify high risk for sudden cardiac death or fatal arrhythmias and to optimize treatment strategies in the clinical setting. ^{11}C-hydroxyephedrine (^{11}C-HED) and ^{123}I-metaiodobenzylguanidine (^{123}I-MIBG) are used for assessing presynaptic sympathetic neuronal function. Nakajima et al. from Kanazawa University Hospital (Japan), Diagram Consulting (Kihei, HI), Hakodate Goryoukaku Hospital (Japan), Obihiro-Kosei Hospital (Japan), and Saiseikai-Futsukaichi Hospital (Tsukushino, Japan) reported on "Prediction of heart failure death based on a 2-year cardiac mortality risk model: Reclassification analysis compared with conventional variables" [366]. The 2-year cardiac mortality risk model, including age, New York Heart Association class, left ventricular ejection fraction, and late heart-to-mediastinum ratio (HMR; assessed by ^{123}I-MIBG uptake) were compared on receiver operating characteristic (ROC) analysis in 402 patients with chronic heart failure. ROC analysis of the 2-year cardiac mortality risk model showed a higher area-under-the-curve value (0.89), indicating better diagnostic accuracy for predicting death from heart failure than univariate models with ^{123}I-MIBG HMR, B-type natriuretic peptide/N-terminal pro B-type natriuretic peptide, or estimated glomerular filtration rate. This is an important clinical study, and it will be interesting to see the results of similar data analyses in patient populations from Europe and/or the United States.

Aikawa et al. from Hokkaido University and Hokkaido University Graduate School of Medicine (Hokkaido and Sapporo, Japan) reported that "Regional myocardial sympathetic denervation is associated with systolic dysfunction independently of myocardial scar in heart failure" [368]. They used ^{11}C-HED PET, which provides high-quality images with quantitative parameters, including retention index as shown in Figure 11. Although the ^{11}C-HED global retention index was correlated with left ventricular ejection fraction and extent of late gadolinium enhancement, a stepwise decrease in regional ^{11}C-HED retention index was also seen with decreasing wall

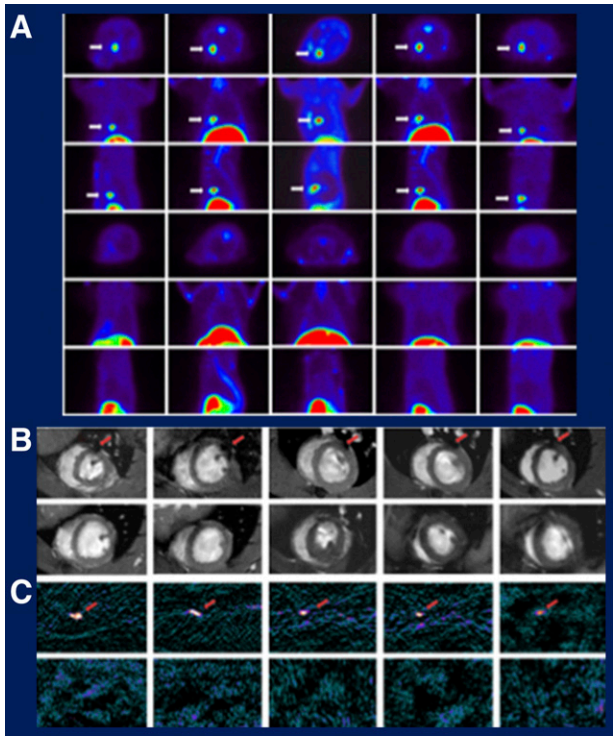

FIGURE 10. Trimodality in vivo reporter gene imaging for monitoring transplanted stem cells in rats after acute myocardial infarction. A: ^{18}F-5-fluoro-*N*-(2-[diethylamino]ethyl)picolinamide (^{18}F-FPN) PET imaging at (left to right) days 1, 7, 14, 21, and 28 after implantation, showing (top to bottom) transverse, coronal, and sagittal views of tyrosinase reporter gene bone-marrow mesenchymal stem cells (TYR-MSCs) and coronal and sagittal views of control mesenchymal stem cells (MSCs). B: MR of (top) TYR-MSCs and (bottom) MSCs at days 1, 7, 14, 21, and 28 after implantation. C: Photoacoustic imaging (PAI) of (top) TYR-MSCs and (bottom) MSCs at days 1, 7, 14, 21, and 28 after implantation. Although clear signals were seen with PET, MR, and PAI (arrows), PET illustrated the best and most persistent positive imaging.

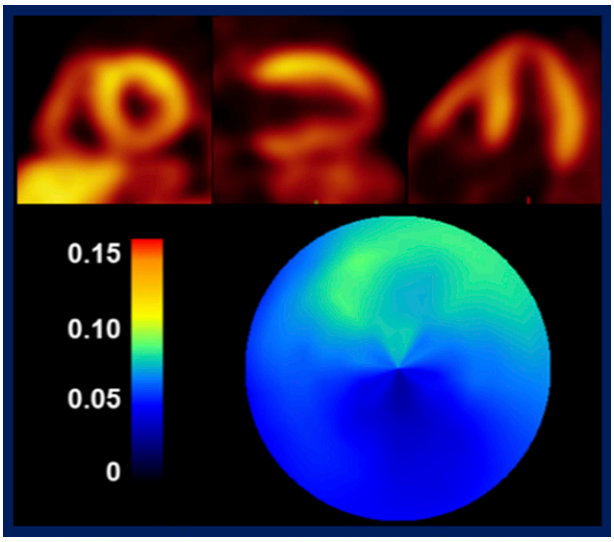

FIGURE 11. Representative ^{11}C-hydroxyephedrine (^{11}C-HED) PET images with regional retention index on a polar map in a patient with cardiac amyloidosis. Excellent image quality demonstrated regional reduction of ^{11}C-HED uptake in inferior regions, with global reduction of retention index on quantitative analysis.

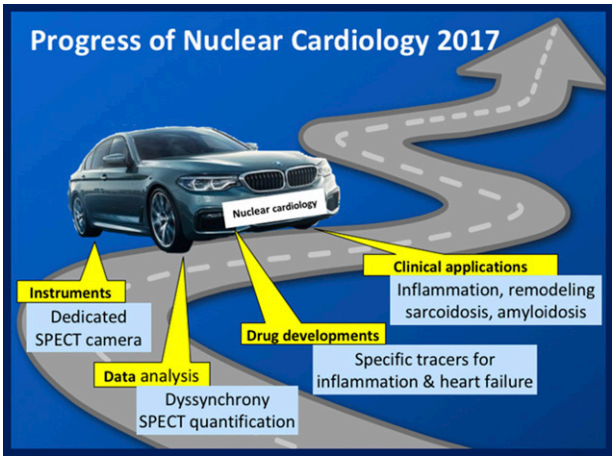

FIGURE 12. Progress of nuclear cardiology in 2017. Four major elements drove nuclear medicine and nuclear cardiology forward. The major targets in each element in 2017 are shown in light blue.

thickening and increasing late gadolinium enhancement. This is the first study indicating regional sympathetic denervation as a novel indicator of myocardial damage in heart failure.

Methodologic Challenges

A number of reports highlighted new applications of PET and cardiac-dedicated SPECT cameras for cardiovascular nuclear medicine. Renaud et al. from the Ottawa Heart Institute (Canada) reported on "Quantification of myocardial blood flow with ^{11}C-HED positron emission tomography imaging" [230]. They measured HED K_1 values with a single-compartment model to compare with myocardial blood flow as assessed by ^{11}C-acetate PET. After correction of the extraction fraction based on the Renkin–Crone capillary model, flow as assessed with HED correlated nicely with that assessed by ^{11}C-acetate. The authors concluded that ^{11}C-HED PET imaging may be used for myocardial blood flow quantification, allowing for simultaneous measurement of sympathetic innervation and myocardial blood flow in a single scan. Further study is warranted to enable wide applications of this elegant technique in patients with heart failure.

Several key presentations for assessing myocardial blood flow using cadmium-zinc-telluride (CZT) SPECT cameras were introduced last year at SNMMI. This year Ko, from National Taiwan University Hospital (Taipei), and Wu from Far Eastern Memorial Hospital (New Taipei City, Taiwan), reported on "Feasibility of absolute flow quantification using dynamic thallium-201 myocardial perfusion SPECT on a CZT camera: A preliminary study" [228]. They used thallium instead of a ^{99m}Tc-labeled perfusion agent, because the former offers better extraction fraction and thus better quantification of myocardial blood flow. The coronary flow reserve assessed by dynamic SPECT adds an incremental value to the summed stress score on stress perfusion SPECT in detecting obstructive coronary artery disease. This is a preliminary result, but if this parameter is readily available with the current method, a wide clinical application is warranted not only for diagnosis but also for severity assessment and monitoring in a variety of treatments for coronary artery disease. However, this study requires 2 separate injections of ^{201}Tl, and, therefore, may raise concerns about radiation dose.

Conclusion

I believe that 4 major elements are driving nuclear medicine forward today: instrument development, data analysis improvement, drug development, and new clinical applications (Fig. 12). These elements constitute 4 "wheels" that provide balanced and safe movement forward. The situation is similar in nuclear cardiology, as described in my previous Annual Highlight talk in 2016. In the 2017 nuclear cardiology sessions, we saw dedicated CZT cameras and SPECT blood flow measurement as examples of instrumentation and data analysis development. Dyssynchrony studies were also a focus this year, mainly because of research integrating echocardiography and MR imaging into nuclear studies. Molecular imaging with a variety of new agents remains a focus of both translational and clinical research. Molecular imaging has recently been used for assessing inflammation and heart failure. In addition, a number of new clinical applications have been introduced for characterizing vulnerable plaque, remodeling, cardiac sarcoidosis, and amyloidosis. In particular, many high-quality abstracts were presented this year in the areas of atherosclerosis and sarcoidosis. With continued development and integration of these 4 elements, the benefits of nuclear cardiology are likely to grow and expand in the future.